

Article

The Distribution and Severity of Corrosion Damage at Eight Distinct Zones of Metallic Femoral Stem Implants

Roohollah Milimonfared ¹, Reza H. Oskouei ¹ , Mark Taylor ¹ and Lucian B. Solomon ^{2,3,*}

¹ The Medical Device Research Institute, College of Science and Engineering, Flinders University, Clovelly Park, SA 5042, Australia; sina.milimonfared@flinders.edu.au (R.M.); reza.oskouei@flinders.edu.au (R.H.O.); mark.taylor@flinders.edu.au (M.T.)

² Department of Orthopaedics and Trauma, Royal Adelaide Hospital, Adelaide, SA 5000, Australia

³ Centre for Orthopaedic & Trauma Research, University of Adelaide, Adelaide, SA 5000, Australia

* Correspondence: bogdan.solomon@sa.gov.au; Tel.: +61-8-70741997

Received: 3 October 2018; Accepted: 17 October 2018; Published: 18 October 2018



Abstract: Metallic taper junctions of modular total hip replacement implants are analysed for corrosion damage using visual scoring based on different granularity levels that span from analysing the taper holistically to dividing the taper into several distinct zones. This study aims to objectively explore the spatial distribution and the severity of corrosion damage onto the surface of metallic stem tapers. An ordinal logistic regression model was developed to find the odds of receiving a higher score at eight distinct zones of 137 retrieved stem tapers. A method to find the order of damage severity across the eight zones is introduced based on an overall test of statistical significance. The findings show that corrosion at the stem tapers occurred more commonly in the distal region in comparison with the proximal region. Also, the medial distal zone was found to possess the most severe corrosion damage among all the studied eight zones.

Keywords: corrosion; metallic implants; taper junction; regression; total hip arthroplasty

1. Introduction

Despite the clinical benefits of modularity in total hip replacement (THR) implants, modular interfaces such as head-neck taper junction sustain mechanically assisted crevice corrosion due to relative micro-motions at the metallic interface and also the presence of corrosive body fluid [1,2]. Previous studies [3–5] have reported that the solid and soluble wear debris and corrosion products released from the head-neck junction may elicit untoward host body reactions such as osteolysis, peri-prosthetic fracture, and metallosis. Depending on the intensity of these postoperative complications, revision surgeries may be needed to replace failed prostheses.

Through large-scale retrieval studies, the surface damage sustained by retrieved implants is assessed, and possible associations between several implant/patients factors and the extent/location of the damage are investigated. The severity of the damage is quantified by using visual scoring methods [6,7]. To date, many studies have applied these methods (with or without modifications) to various modular junctions [7–10]. Upon scoring the damage, each study employs a causal-explanatory statistical modelling to investigate the effect of a particular set of factors (predictors) on the damage score.

In the head-neck junction, stems have a tapered geometry which can be divided into several zones (e.g., anterior, medial, posterior, and lateral quadrants). A deeper level of score granularity can provide more details about the severity and spatial distribution of damage. Distribution of the

corrosion damage over the distinct zones of tapers has been investigated by a limited number of studies [8,11–19].

The number of zones scored at stem tapers has seldom gone beyond four (anterior, medial, posterior, and lateral quadrants). One reason for that could be the complexity of conducting pairwise comparisons within the groups of zone factor. With four zones, six combinations (order disregarded) would be required. If it is desired to consider the distal and proximal regions of each quadrant as well, 28 (i.e., $\frac{8!}{(8-2)! \times 2!}$) pairwise comparisons would be required to investigate the damage thoroughly. The studies that scored the distal and proximal regions separately have observed different damage patterns within these regions [15,18,19]. Therefore, it is necessary to look at stem taper zones with a higher level of granularity in order to explore whether any significant difference exists between the distal and proximal regions of the quadrants.

This study introduces a method for addressing this gap. Using this approach, eight individual corrosion scores are assigned to eight distinct zones of each metallic stem taper. Next, an ordinal logistic regression (OLR) model is used to quantitatively compare the severity of corrosion damage at these eight zones.

2. Materials and Methods

2.1. Retrieved Implants Information

This study was approved by the Southern Adelaide Clinical Human Research Ethics Committee (Reference No. 485.13); 137 total hip replacement implants retrieved between 1995 and 2015 at the Royal Adelaide Hospital (RAH), Adelaide, Australia were selected. The selection was limited to include only detached head-neck junctions so that the stem tapers were accessible for assessment. The retrieved implants had been disinfected by immersing in 70% ethanol for four days followed by a 4% Biogram solution (polyphenolic disinfectant and detergent with 18% phenol) for 48–72 h. Biologic debris (blood or proteinaceous films) had been removed using a cotton bud without abrasion. The stem tapers, selected for this research, were further cleaned with acetone followed by a gentle wipe with a soft nylon brush. Eleven implant/patient factors were retrieved from Our Patient Management and Outcomes Database (OPMOD) of the RAH. Table 1 provides the demography of these categorical and continuous factors. The missing information associated with each factor supplements the quantity of each factor to add up to 137. This study only looks at the distribution and severity of corrosion. Therefore, the missing patient and implant information did not pose any concern.

Table 1. Demographics of the selected retrievals for this study.

Predictor	Quantity (% Frequency)	Median	Range
Head Material			
CoCr	60 (43.8)		
Stainless Steel (SS)	7 (5.1)		
Ceramic	8 (5.8)		
Stem Material			
CoCr	54 (39.4)		
Stainless Steel (SS)	41 (29.9)		
Titanium	31 (22.6)		
Stem Fixation			
Cemented	76 (55.5)		
Cementless	50 (36.5)		
Gender			
Female	57 (45.2)		
Male	69 (54.8)		
Stem Taper			
12/14	52 (38.0)		
V40	19 (13.9)		
9/10	12 (8.8)		

Table 1. Cont.

Predictor	Quantity (% Frequency)	Median	Range
6°	8 (5.8)		
C-TAPER	8 (5.8)		
TYPE 1	2 (1.5)		
11/13	3 (2.2)		
10/12	1 (0.7)		
Joint Side			
Right	69 (54.8)		
Left	57 (45.2)		
Head Diameter (mm)		28	22–55
Time to Revision (year)		6	0–35
Weight (kg)		77	51–178
Age at Primary (year)		63.5	22–85

2.2. Visual Assessment of Corrosion Damage

The Goldberg's scoring method [7] was used to inspect and rate corrosion on the stem tapers (Table 2). Based on this method, eight distinct zones of the retrieved stem tapers were scored individually. Fretting wear was not scored because it has been reported by several studies that fretting may be masked by corrosion damage; and therefore, hard to visually identify [14,15,19,20].

Table 2. Visual criteria for scoring corrosion damage.

Score	Visual Criteria
1 (None)	No Visible Corrosion
2 (Mild)	<30% Surface Discoloured/Dull
3 (Moderate)	>30% Surface Discoloured/Dull or <10% Containing Black Debris, Pits or Etch Marks
4 (Severe)	>10% of Surface Containing Black Debris, Pits, or Etch Marks

Also, it is thought that the severity of fretting in Goldberg's method cannot be measured consistently because the pitch of the machined threads over the taper surface varies among different stem designs [14,21]. Lastly, fretting scars can be mixed up with scratches caused by attaching or detaching the head intraoperatively [7,12,21].

In order to have a consistent scoring, one trained investigator (RM) evaluated the damage. The stem tapers were visually scored twice in a random order. Each stem taper was photographed and eight zones (posterior-distal (PD), posterior-proximal (PP), medial-distal (MD), medial-proximal (MP), anterior-distal (AD), anterior-proximal (AP), lateral-distal (LD), and lateral-proximal (LP)) were identified according to our previous study [22]. Figure 1 displays an exemplary taper for each score level.



Figure 1. Corrosion damage scores of 1 through 4 for stem tapers.

2.3. Statistical Analysis

In this study, SPSS (version 25) was used for the statistical analysis and a p -value of <0.05 was determined as the level of statistical significance. Weighted kappa (κ_W) with quadratic weights was run to determine the single-observer repeatability of the corrosion scores. A confusion matrix was established to quantify the disagreements. For quadratic weights, the further away a disagreement was from the perfect agreement, the more harshly that disagreement is considered. The strength of agreement based on the magnitude of the weighted kappa (κ_W) was interpreted according to the guideline reported in Landis et al. [23].

Having an ordinal dependent variable (DV) as the response, OLR was employed to capture the ordered nature of the DV levels. The OLR model in this study uses cumulative logits. Selection of cumulative logits against other models (e.g., adjacent or continuation categories) was due to the interest of this study to use the entire response scale regardless of the score level.

Consequently, the cumulative odds OLR came with proportional odds constraint to ensure the regression lines across the DV levels are parallel. This OLR model divides the categories of the ordinal DV to run cumulative logits, as demonstrated in Table 3.

Table 3. An ordinal dependent variable (DV) with four levels giving three cumulative probabilities and consequently logits.

Binomial Regression	Event Category	Non-Event Categories
1	Probability (score ≤ 1) “none”	Probability (score > 1) “mild”, “moderate”, and “severe”
2	Probability (score ≤ 2) “none” and “mild”	Probability (score > 2) “moderate” and “severe”
3	Probability (score ≤ 3) “none”, “mild”, and “moderate”	Probability (score > 3) “severe”

With a four-level DV, this OLR model outputs three binomial logistic regressions, according to Equations (1)–(3) that predict the probability of being classified into the ‘lower’ categories as opposed to the ‘higher’ categories for each dichotomization of the ordinal DV based on the cumulative probabilities.

$$\text{logit}(\text{success}) = \ln \left(\frac{\text{Prob}(\text{score} \leq 1)}{\text{Prob}(\text{score} > 1)} \right) \quad (1)$$

$$\text{logit}(\text{success}) = \ln \left(\frac{\text{Prob}(\text{score} \leq 2)}{\text{Prob}(\text{score} > 2)} \right) \quad (2)$$

$$\text{logit}(\text{success}) = \ln \left(\frac{\text{Prob}(\text{score} \leq 3)}{\text{Prob}(\text{score} > 3)} \right) \quad (3)$$

2.3.1. The Ordinal Logistic Regression (OLR) Assumptions

Before deploying an OLR model, four assumptions (constraints) needed to be considered to ensure the validity of the results. The first assumption mandates the DV (visual scores) having an ordinal level of measurement which is valid here. Under the second assumption, there should be at least one independent variable (IV) that is continuous, ordinal or categorical (including dichotomous variables) which is valid as well.

The other two assumptions are related to the characteristics of the data. The third assumption mandates no multi-collinearity between the IVs. It was implemented by incorporating collinearity diagnostic under linear regression which returns the variance of inflation factor (VIF). VIF indicates to what extent a particular IV contributes to multi-collinearity issues within the dataset. In this study, VIF values beyond 10 were considered as having multi-collinearity as a rule of thumb.

The fourth assumption checks for having proportional odds. Here, the test of parallel lines was used to compare the fit of the proportional odds model to a model with varying slope coefficients. It was desired not to reject the null hypothesis that states the slope coefficients are the same across the three cumulative regression models. If true, the effect of each IV will be identical at each cumulative logit which is desired here.

2.3.2. Overall Parameter Estimates

As pointed out earlier, the type of OLR model used in this study produces an equation for each cumulative logit. As there are four categories of the DV, three cumulative logits (Equations (1)–(3)) are expected. Also, the assumption of proportional odds constrains the slope coefficients to be the same for all the three equations, so it is just going to be the thresholds that may vary between the three equations.

Since changes in log odds do not have much intuitive meaning, the ratio of the odds between any two categories or a unit change in a numerical IV is reported. The odds ratio (OR) was calculated as the exponential of the log odds of the slope coefficient. Also, the 95% confidence intervals of the OR and the significance levels are reported.

Unlike the numerical and dichotomous IVs, zone, as a polytomous IV, demands additional calculations to complete an overall test of statistical significance. To exhaust the entire pairwise comparison of the categories, one category was taken as the reference, and the rest were compared with that as primary categories. In each significance test, each zone had to be recoded into a new variable with the desirable reference category being coded as the last category (highest level).

3. Results

For the assessment of intra-observer repeatability, the weighted kappa (κ_W) with quadratic weights indicated a statistically significant agreement, $\kappa_W = 0.64$ (95% CI, 0.59 to 0.69), $p < 0.001$ between the two sets of scores. According to [23], the strength of the agreement was classified as good. Before using the OLR model, preliminary data analysis was carried out by looking at frequency histograms of the scores in different zones. Using various bin sizes and definitions, a number of different histograms were generated to graphically summaries the distribution of scores across the eight taper zones.

3.1. Distribution of Corrosion Scores

Visual scoring of the 137 stem tapers across the eight zones resulted in 1096 corrosion scores. Table 4 summarizes the frequency of each score level. Score level 2 had the highest quantity (512) while the lowest quantity (51) belonged to score level 4.

Table 4. The quantity of the zones having each score level.

Score	Quantity (%)
1	359 (32.8)
2	512 (46.7)
3	174 (15.9)
4	51 (4.7)

Figure 2 illustrates the distribution of the corrosion scores at each zone. This figure can be used to compare the variability of each score level across the eight zones. The values are the percentage of each score out of 137 in every zone (the percentages in each zone add up to 100%). Score levels 1 through 4 stood in the first place at zones PP, AD, MD, and MP, respectively.

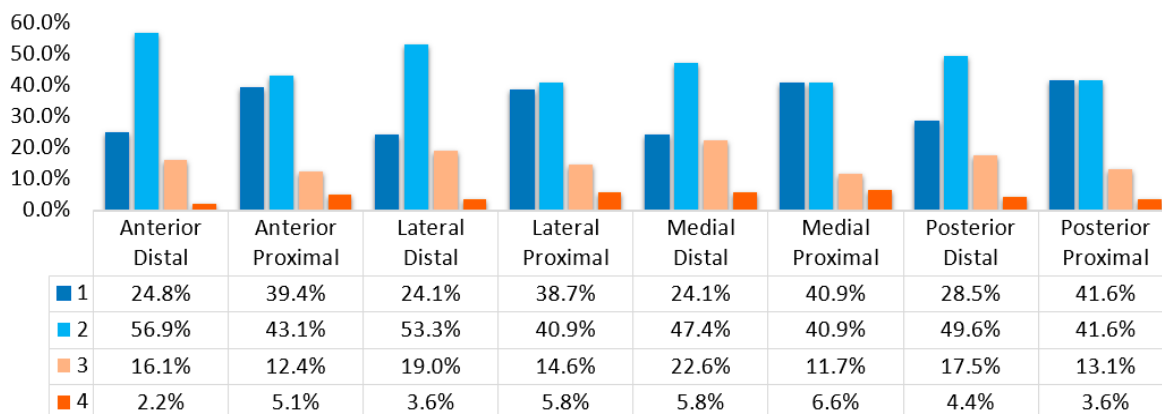


Figure 2. Distribution of corrosion score levels across the entire eight stem taper zones of the 137 retrieved implants.

Considering the unbalanced score levels, the first two score levels that are higher in quantity (i.e., 359 and 512) always show higher percentages compared with score levels 3 and 4 within each zone.

To better compare the severity of damage across the zones, two more configurations of scores (by combining the original score levels) were also explored. The first configuration groups the first and the last two score levels into low and high groups, respectively. Figure 3 visualizes this configuration and compares each score group across the eight zones.

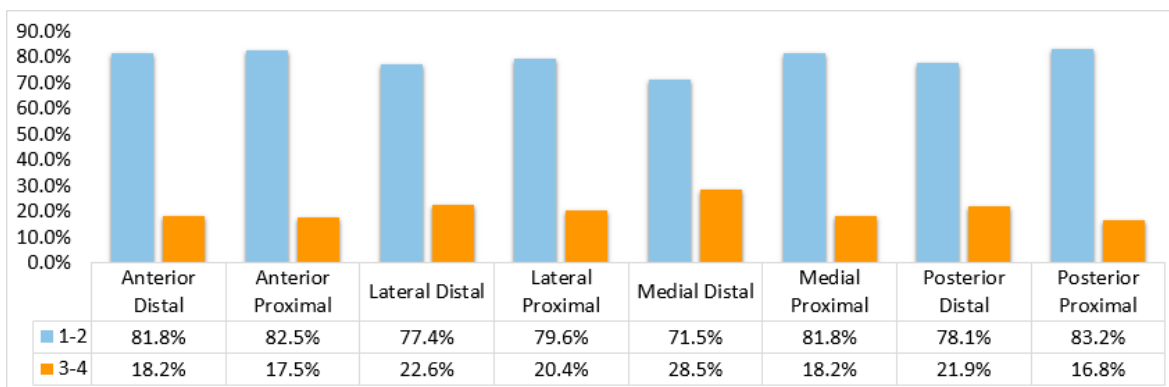


Figure 3. The quantity of the double score levels at each zone (scores 1 and 2 versus scores 3 and 4 combined).

As expected, the low score group which comprises (359 + 512) scores has a higher frequency compared with the high score group (174 + 51). This configuration can better show which zones have more severe corrosion damage (for example, MD and LD zones). Also, at zones MD and PP, the smallest and largest gaps between these two combined score levels were observed.

The third configuration preserves score level 1 and combines the other three score levels to form two new score groups of intact and corroded stem tapers. Figure 4 illustrates the frequencies of these two score groups.

The medial distal zone had the largest difference between these two score groups which confirms that this particular zone is most damaged. Also, the posterior-proximal zone had the smallest difference between the two score groups (thus least damaged). As a key finding, the distal regions of the four quadrants showed more corrosion damage compared with the proximal regions.

These findings from the histogram can shed light on the likely outcome of the OLR model. In particular, when the number of DV levels are higher, cumulative logits models may become

infeasible. Histograms can determine which score levels are more important to be compared via using other types of OLR models such as adjacent categories.

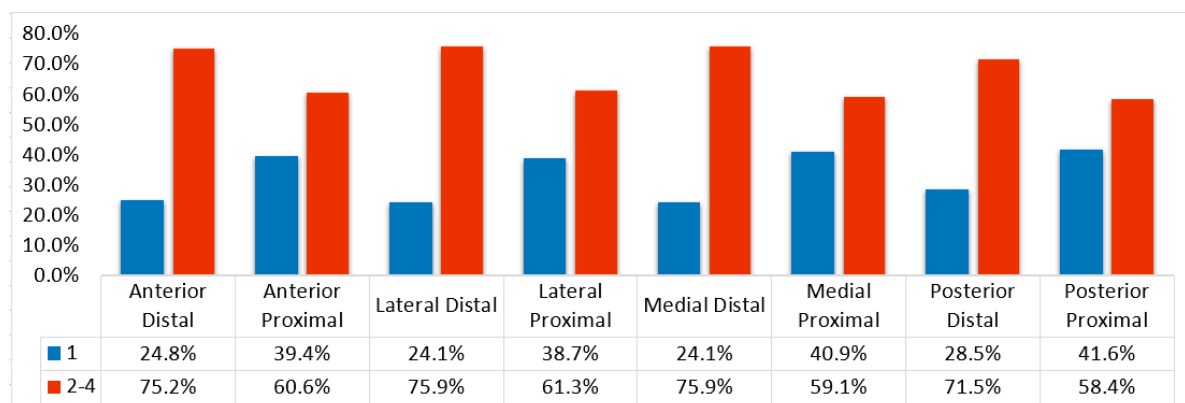


Figure 4. Distribution of corroded stem tapers against the intact group.

3.2. Comparison of Corrosion in the Zones

Cumulative odds OLR with proportional odds was employed to conduct pairwise comparisons between the zones. First, it was established whether zone is statistically significant overall. From the test of model performed on SPSS, zone was observed to be a statistically significant ($p = 0.002$) predictor of corrosion scores in this univariate regression model.

Since no specific zone was preferential to investigate, 28 pairwise comparisons had to be undertaken which incurred additional calculations to obtain the overall omnibus statistical test. Table 5 summarizes the OR, p -values, and confidence intervals. Significant OR values are highlighted in grey. In this table, each zone has been used seven times either as the primary or reference (inside brackets) group to exhaust the combinations. OR values below 1 indicate that for the primary category, the odds of having a higher corrosion score is lower than that of the reference category.

Table 5. The odds of observing a higher corrosion score at a primary zone compared with a reference zone.

Zone Pair	OR	p -Value	CI ($p < 0.05$)	
AD (AP)	1.493	0.077	0.957	2.329
AD (LD)	0.882	0.577	0.566	1.372
AD (LP)	1.365	0.169	0.876	2.128
AD (MD)	0.755	0.212	0.485	1.175
AD (MP)	1.524	0.063	0.977	2.378
AD (PD)	0.998	0.993	0.641	1.554
AD (PP)	1.634	0.031	1.047	2.551
AP (LD)	0.590	0.020	0.379	0.921
AP (LP)	0.914	0.693	0.586	1.427
AP (MD)	0.505	0.003	0.324	0.789
AP (MP)	1.021	0.928	0.654	1.594
AP (PD)	0.668	0.076	0.429	1.043
AP (PP)	1.094	0.692	0.701	1.709
LD (LP)	1.549	0.054	0.993	2.414
LD (MD)	0.856	0.490	0.550	1.331
LD (MP)	1.729	0.016	1.108	2.697
LD (PD)	1.132	0.583	0.727	1.762
LD (PP)	1.853	0.007	1.187	2.894
LP (MD)	0.553	0.009	0.355	0.862

Table 5. Cont.

Zone Pair	OR	<i>p</i> -Value	CI (<i>p</i> < 0.05)	
LP (MP)	1.116	0.628	0.715	1.742
LP (PD)	0.731	0.167	0.469	1.140
LP (PP)	1.197	0.429	0.767	1.869
MD (MP)	2.019	0.002	1.294	3.152
MD (PD)	1.322	0.216	0.850	2.058
MD (PP)	2.165	0.001	1.386	3.382
MP (PD)	0.655	0.062	0.420	1.022
MP (PP)	1.072	0.760	0.686	1.675
PD (PP)	1.637	0.030	1.049	2.556

The reciprocal of odds ratios can be calculated to compare a reference group with a primary group. To compare the severity of corrosion across the entire eight zones, the odds ratios were sorted and plotted (Figure 5). The red and blue bars indicate the significant and insignificant OR values, respectively. An OR equal to 1 indicates equal odds of observing a higher corrosion score at the primary and reference zone groups. By moving away from unity, the odds ratios that are first insignificant later on become significant. The speed by which this transition takes place is a function of the presumed statistical significance level.

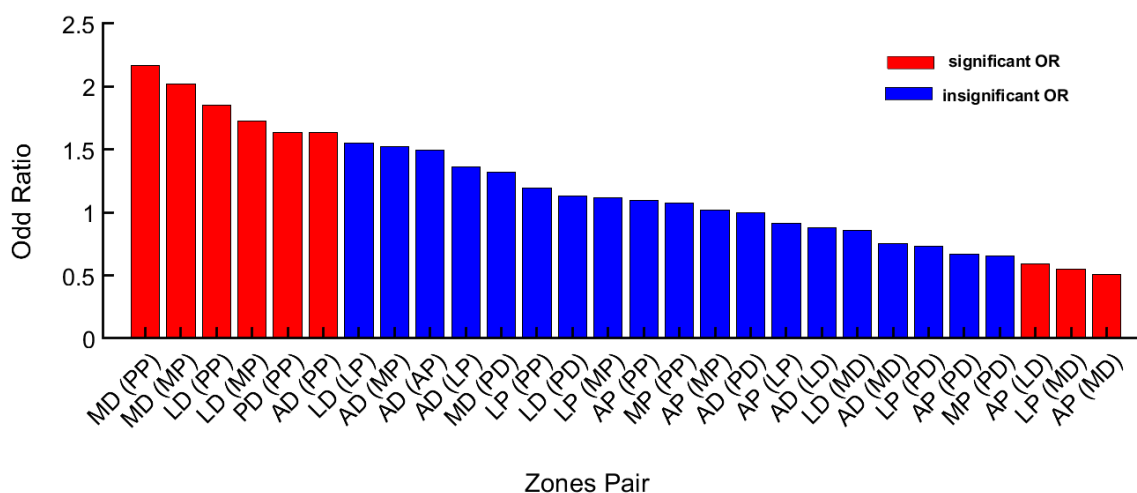


Figure 5. The 28 odds ratios sorted and colour-coded for 28 pairwise comparisons.

The severity of corrosion at each zone with respect to the other zones was assessed based on its corresponding OR values. For each zone, Table 5 has provided seven OR values wherein that particular zone appears as either primary or reference.

Table 6 sorts the eight zones from the least to the most severely damaged according to the value of C1 + C2. This value quantifies how many times each zone had a higher likelihood of damage compared with the other seven zones throughout the 28 pairwise comparisons. C1 indicates how many time a particular zone, as the primary, had an OR value above 1, while C2 indicates how many times that same zone, as the reference, had an OR value below 1. Therefore, both C1 and C2 reflects the frequency of each zone appearing as more severely damaged with respect to the other zones.

Table 6. The frequency of each zone showing statistically significant odds ratio (OR).

Zone	C1	C2	C1 + C2
Posterior Proximal (PP)	0	0	0
Medial Proximal (MP)	1	0	1
Anterior Proximal (AP)	2	0	2

Table 6. Cont.

Zone	C1	C2	C1 + C2
Lateral Proximal (LP)	2	1	3
Anterior Distal (AD)	4	0	4
Posterior Distal (PD)	1	4	5
Lateral Distal (LD)	4	2	6
Medial Distal (MD)	3	4	7

Zones PP and MD were identified having the least and highest severity of corrosion. Interestingly, proximal and distal regions were found to be grouping together in this table with the distal region showing more damage compared with the proximal region across the four quadrants in the studied stem tapers.

4. Discussion

Eight distinct zones of the stem tapers including anterior-distal, anterior-proximal, medial-distal, medial-proximal, posterior-distal, posterior-proximal, lateral-distal, and lateral-proximal were scored and statistically compared to identify the zone(s) with the most severe corrosion damage in the retrieved implants studied in this work. It is noted that there are several studies in the literature that chose to score stem tapers holistically, not locally [9,10,24–26].

Within the studies [11,12,15–19] that scored stem tapers locally, the pools of implants had a limited diversity in terms of implant properties (e.g., head diameter, articulation type, and stem design). Therefore, it was deemed necessary to explore whether a similar distribution of corrosion damage can be seen in a more heterogeneous pool of implants.

To the best of our knowledge, there are only two studies [18,19] in the literature that, similar to this work, have assigned eight local scores to the stems with the rest using lower numbers of zones. In those two studies, one did not compare the scores between the zones [18]. The other compared the four quadrants, and the two distal and proximal regions separately in terms of corrosion severity and did not determine which zone(s) had the most severe damage [19].

Routine causal-explanatory statistical analyses require only one score as the descriptor of damage for each implant. The majority of these studies have chosen to combine the local scores by calculating an overall value [8,11–14]. This approach has led to the presumption that this global score is a continuous variable; and, thus, the statistical analyses for continuous variables have been utilised. Analysing a continuous variable with an interval or ratio level of measurement is generally less complex in nature. However, an increased number of levels in the global score does not necessarily imply a known “distance” between the score levels. Therefore, this approach was treated with suspicion in this study and was not adopted.

Here, the corrosion scores were analysed using a univariate OLR model, and the odds ratios along with their *p*-values were reported. Since there was no particular hypothesis about the relative level of corrosion at the eight zones, 28 pairwise comparisons were carried out to exhaust the entire pairwise comparison of the zones. The distal region of the medial quadrant was found to have the highest odds of receiving a higher corrosion score which is aligned with the previous findings in the literature that identified the distal region [19,20,27] and the medial quadrant [7,10,16,28] having the highest corrosion scores. Also, this study shows that the distal region of all the four quadrants had more corrosion damage in comparison with the proximal region of those quadrants. Therefore, it was found that, regardless of the quadrant, corrosion damage is more present distally than proximally.

Generally, the higher severity of wear or corrosion at a specific zone has been attributed to several factors such as increased micro-motions at the interface, head or stem materials, head diameter, high friction moments, and poor lubrication of the bearing articulation. While some act as root causes, the others play the role of causal factors. Also, damage at the head-neck taper junction usually appears

as a combination of wear and corrosion mechanisms. Some of these factors may only contribute to a specific mode of damage, while others may contribute towards a set of damage mechanisms.

In a retrieval study of 231 implants [7] the stem tapers received four fretting and corrosion scores corresponding to the four quadrants. The medial and lateral scores were observed to be significantly higher than the scores at the other two quadrants (posterior and anterior). This was explained to be due to a higher likelihood of micro-motions between the head and neck about an axis in the sagittal plane. Similar to the present study, the pool of implants in this work had a wide diversity, and higher corrosion scores at the medial quadrant suggest that it could be a phenomenon independent of the included patient and implant factors.

Wilson et al. [29] explained how at the double-tapered cone design of Profemur Z, the proximal end of the neck experiences an almost pure compression and shear loading. High frictional moments at taper junctions were related to poor lubrication of the articulation interfaces by another study [30].

The medial quadrant was identified to have higher corrosion scores in a retrieval study of 52 S-ROM components [16]. It was hypothesised that greater micro-motions at this quadrant could result in a more frequent disruption of the passive oxide layer; and consequently, more severe corrosion damage. Similar to the conclusion of the Wilson et al. [29] study, they reported that this region is generally under a compression-loading regime. A computational modelling of the stem taper stresses paired with large diameter heads confirmed this hypothesis after witnessing maximum levels of principal stresses at the medial quadrant [31]. In that work, a 3D model of a 12/14 titanium taper was paired with cobalt-chromium and alumina heads. Increasing the head diameter increased this quadrant's stresses distal to the junction significantly. It was highlighted that the pairing of a small taper and a large head leads to a larger moment arm transmitting a higher force to a small surface area which facilitates tribo-corrosion.

A relatively higher amount of load and stress at the medial quadrant causes elastic strains which appear as surface compression. This condition may lead to micro-motions of approximately 5 to 40 μm [32] which in turn may result in abrasion or fracture of the oxide layer. The subsequent changes in the metal surface potential and the continuous re-passivation of the oxide layer change the chemistry of the crevice solution. Ultimately, the deaeration and pH decrease of the solution initiate crevice corrosive attacks [33,34]. Crevice corrosion has been reported to occur near the bore opening which may explain observing more severe corrosion at the distal region [35].

Besides micro-motions, galvanic corrosion at this interface due to using mixed metal components is a potential source of material loss. In this study, 18 (13.1%) implants had mixed head and stem materials, whereas 45 (32.8%) had similar materials. Therefore, galvanic corrosion cannot be nominated as the sole mechanism of corrosion.

These studies have used relatively homogenous pools of implants, yet they observed higher levels of corrosion at the medial quadrant or distal zones of stem tapers. Based on the findings of the present study which shows that the distal region of the medial quadrant sustains the most severe corrosion damage, it is understood that this particular zone is most severely damaged versus all the other zones regardless of the properties and patient characteristics of the investigated pool of implants.

5. Conclusions

This study introduces a method to statistically compare the severity of corrosion damage at eight distinct zones of stem tapers. A pool of 137 retrieved total hip replacement implants was visually scored at the head-neck junction for corrosion damage using Goldberg's method. An OLR model with proportional odds was used to determine the odds of observing a higher score at a primary zone compared with a reference zone. The findings of this study can be highlighted as below:

- The corrosion score level 2 was observed having the highest frequency (46.7%).
- Posterior-proximal and medial-distal were identified as the zones with the least and most severity of corrosion.

- Interestingly, the proximal and distal regions were found to be grouping together with the distal region showing more damage in comparison with the proximal region of the four quadrants.
- Out of the 28 pairwise comparisons of these eight zones, nine pairs of zones were identified to be significantly different regarding corrosion damage. This observation objectively shows the high diversity in corrosion damage across these zones.
- Retrieval studies of taper junctions are, therefore, recommended to score the zones separately and avoid adding up local scores to be used with an interval or ratio level of measurement.

Author Contributions: R.M. studied the implants, conducted the statistical analysis, discussed the results and drafted the manuscript. R.H.O., M.T. and L.B.S. supervised and contributed to all the project tasks including revising and writing of the paper.

Funding: This research received no external funding.

Acknowledgments: The authors would like to acknowledge the support through an Australian Government Research Training Program Scholarship for Roohollah Milimonfared's PhD. The authors also thank the Department of Orthopaedics and Trauma, Royal Adelaide Hospital (Adelaide, Australia), and in particular, Kerry Costi and Roumen Stamenkov for their assistance in accessing the retrieved implants.

Conflicts of Interest: The authors have no conflicts of interest to declare.

References

1. Hussenbocus, S.; Kosuge, D.; Solomon, L.B.; Howie, D.W.; Oskouei, R.H. Head-neck taper corrosion in hip arthroplasty. *BioMed Res. Int.* **2015**, *2015*, 758123. [[CrossRef](#)] [[PubMed](#)]
2. Oskouei, R.H.; Barati, M.R.; Farhoudi, H.; Lucian, M.T.; Solomon, B. A new finding on the in-vivo crevice corrosion damage in a CoCrMo hip implant. *Mat. Sci. Eng. C* **2017**, *79*, 390–398. [[CrossRef](#)] [[PubMed](#)]
3. Jacobs, J.J.; Cooper, H.J.; Urban, R.M.; Wixson, R.L.; Della Valle, C.J. What do we know about taper corrosion in total hip arthroplasty? *J. Arthroplasty* **2014**, *29*, 668–669. [[CrossRef](#)] [[PubMed](#)]
4. Cooper, H.J.; Della Valle, C.J.; Berger, R.A.; Tetreault, M.; Paprosky, W.G.; Sporer, S.M.; Jacobs, J.J. Corrosion at the head-neck taper as a cause for adverse local tissue reactions after total hip arthroplasty. *J. Bone Jt. Surg. Am.* **2012**, *94*, 1655–1661. [[CrossRef](#)]
5. Vundelinckx, B.J.; Verhelst, L.A.; De Schepper, J. Taper corrosion in modular hip prostheses: Analysis of serum metal ions in 19 patients. *J. Arthroplasty* **2013**, *28*, 1218–1223. [[CrossRef](#)] [[PubMed](#)]
6. Gilbert, J.L.; Buckley, C.A.; Jacobs, J.J. In vivo corrosion of modular hip prosthesis components in mixed and similar metal combinations. The effect of crevice, stress, motion, and alloy coupling. *J. Biomed. Mater. Res.* **1993**, *27*, 1533–1544. [[CrossRef](#)] [[PubMed](#)]
7. Goldberg, J.R.; Gilbert, J.L.; Jacobs, J.J.; Bauer, T.W.; Paprosky, W.; Leurgans, S. A multicenter retrieval study of the taper interfaces of modular hip prostheses. *Clin. Orthop. Relat. Res.* **2002**, *401*, 149–161. [[CrossRef](#)]
8. Hothi, H.S.; Berber, R.; Panagiotopoulos, A.C.; Whittaker, R.K.; Rhead, C.; Skinner, J.A.; Hart, A.J. Clinical significance of corrosion of cemented femoral stems in metal-on-metal hips: A retrieval study. *Int. Orthop.* **2016**, *40*, 2247–2254. [[CrossRef](#)] [[PubMed](#)]
9. Carlson, J.C.H. Femoral stem fracture and in vivo corrosion of retrieved modular femoral hips. *J. Arthroplasty* **2012**, *27*, 1389–1396. [[CrossRef](#)] [[PubMed](#)]
10. Higgs, G.B. Method of characterizing fretting and corrosion at the various taper connections of retrieved modular components from metal-on-metal total hip arthroplasty. Metal-on-metal total hip replacement devices. *ASTM Int.* **2013**, *1560*, 146–156. [[CrossRef](#)]
11. Tan, S.C.; Lau, A.C.; Del Balso, C.; Howard, J.L.; Lanting, B.A.; Teeter, M.G. Tribocorrosion: Ceramic and oxidized zirconium vs cobalt-chromium heads in total hip arthroplasty. *J. Arthroplasty* **2016**, *31*, 2064–2071. [[CrossRef](#)] [[PubMed](#)]
12. Tan, S.C.; Teeter, M.G.; Del Balso, C.; Howard, J.L.; Lanting, B.A. Effect of taper design on trunnionosis in metal on polyethylene total hip arthroplasty. *J. Arthroplasty* **2015**, *30*, 1269–1272. [[CrossRef](#)] [[PubMed](#)]
13. Hothi, H.S.; Berber, R.; Whittaker, R.K.; Bills, P.J.; Skinner, J.A.; Hart, A.J. Detailed inspection of metal implants. *Hip Int.* **2015**, *25*, 227–231. [[CrossRef](#)] [[PubMed](#)]

14. Hothi, H.S.; Matthies, A.K.; Berber, R.; Whittaker, R.K.; Skinner, J.A.; Hart, A.J. The reliability of a scoring system for corrosion and fretting, and its relationship to material loss of tapered, modular junctions of retrieved hip implants. *J. Arthroplasty* **2014**, *29*, 1313–1317. [[CrossRef](#)] [[PubMed](#)]
15. De Martino, I.; Assini, J.B.; Elpers, M.E.; Wright, T.M.; Westrich, G.H. Corrosion and fretting of a modular hip system: A retrieval analysis of 60 rejuvenate stems. *J. Arthroplasty* **2015**, *30*, 1470–1475. [[CrossRef](#)] [[PubMed](#)]
16. Munir, S.; Michael, B.C.; Christina, E.; Anna, S.; William, L.W. Corrosion in modular total hip replacements: An analysis of the head–neck and stem–sleeve taper connections. *Semin. Arthroplasty* **2013**, *24*, 240–245. [[CrossRef](#)]
17. Stamer, C.M. Assessment of Bore-Cone Taper Junctions in Explanted Modular Total Hip Replacements. Master's Thesis, Clemson University, Clemson, SC, USA, 2015.
18. Kao, Y.-Y.J.; Koch, C.N.; Wright, T.M.; Padgett, D.E. Flexural rigidity, taper angle, and contact length affect fretting of the femoral stem trunnion in total hip arthroplasty. *J. Arthroplasty* **2016**, *31*, S254–S258. [[CrossRef](#)] [[PubMed](#)]
19. Triantafyllopoulos, G.K.; Elpers, M.E.; Burket, J.C.; Esposito, C.I.; Padgett, D.E.; Wright, T.M. Otto aufranc award: Large heads do not increase damage at the head-neck taper of metal-on-polyethylene total hip arthroplasties. *Clin. Orthop. Relat. Res.* **2015**, *474*, 330–338. [[CrossRef](#)] [[PubMed](#)]
20. Gonzalez, J.L., Jr. In-Vivo Corrosion and Fretting of Modular Ti-6Al-4V/CO-CR-MO Hip Prostheses: The Influence of Microstructure and Design Parameters. Master's Thesis, Florida International University, Miami, FL, USA, 2015.
21. Kocagöz, S.B.; Underwood, R.J.; Sivan, S.; Gilbert, J.L.; MacDonald, D.W.; Day, J.S.; Kurtz, S.M. Does taper angle clearance influence fretting and corrosion damage at the head–stem interface? A matched cohort retrieval study. *Semin. Arthroplasty* **2013**, *24*, 246–254. [[CrossRef](#)] [[PubMed](#)]
22. Milimonfared, R.; Oskouei, R.H.; Taylor, M.; Solomon, L.B. An intelligent system for image-based rating of corrosion severity at stem taper of retrieved hip replacement implants. *Med. Eng. Phys.* **2018**. [[CrossRef](#)] [[PubMed](#)]
23. Landis, J.R.; Koch, G.G. The measurement of observer agreement for categorical data. *Biometrics* **1977**, *33*, 159–174. [[CrossRef](#)] [[PubMed](#)]
24. Higgs, G.B.; MacDonald, D.W.; Lowell, J.; Padayatil, A.; Mihalko, W.M.; Siskey, R.L.; Gilbert, J.L.; Rimnac, C.M.; Kurtz, S.M. Is corrosion a threat to the strength of the taper connection in femoral components of total hip replacements? *Corrosion* **2017**, *73*, 1538–1543. [[CrossRef](#)]
25. Whittaker, R.K.; Hothi, H.S.; Meswania, J.M.; Berber, R.; Blunn, G.W.; Skinner, J.A.; Hart, A.J. The effect of using components from different manufacturers on the rate of wear and corrosion of the head-stem taper junction of metal-on-metal hip arthroplasties. *Bone Jt. J.* **2016**, *98*, 917–924. [[CrossRef](#)] [[PubMed](#)]
26. Matthies, A.K.; Racasan, R.; Bills, P.; Blunt, L.; Cro, S.; Panagiotidou, A.; Blunn, G.; Skinner, J.; Hart, A.J. Material loss at the taper junction of retrieved large head metal-on-metal total hip replacements. *J. Orthop. Res.* **2013**, *31*, 1677–1685. [[CrossRef](#)] [[PubMed](#)]
27. Langton, D.J.; Sidaginamale, R.P.; Joyce, T.J.; Meek, R.D.; Bowsher, J.G.; Deehan, D.; Nargol, A.V.F.; Holland, J.P. A comparison study of stem taper material loss at similar and mixed metal head-neck taper junctions. *Bone Jt. J.* **2017**, *99*, 1304–1312. [[CrossRef](#)] [[PubMed](#)]
28. Higgs, G.B.; Hanzlik, J.A.; MacDonald, D.W.; Gilbert, J.L.; Rimnac, C.M.; Kurtz, S.M. Is increased modularity associated with increased fretting and corrosion damage in metal-on-metal total hip arthroplasty devices?: A retrieval study. *J. Arthroplasty* **2013**, *28*, 2–6. [[CrossRef](#)] [[PubMed](#)]
29. Wilson, D.A.; Dunbar, M.J.; Amirault, J.D.; Farhat, Z. Early failure of a modular femoral neck total hip arthroplasty component a case report. *J. Bone Jt. Surg. Am.* **2010**, *92*, 1514–1517. [[CrossRef](#)] [[PubMed](#)]
30. Bishop, N.E.; Hothan, A.; Morlock, M.M. High friction moments in large hard-on-hard hip replacement bearings in conditions of poor lubrication. *J. Orthop. Res.* **2013**, *31*, 807–813. [[CrossRef](#)] [[PubMed](#)]
31. Lavernia, C.J.; Iacobelli, D.A.; Villa, J.M.; Jones, K.; Gonzalez, J.L.; Jones, W.K. Trunnion-head stresses in THA: Are big heads trouble? *J. Arthroplasty* **2015**, *30*, 1085–1088. [[CrossRef](#)] [[PubMed](#)]
32. Porter, D.A.; Urban, R.M.; Jacobs, J.J.; Gilbert, J.L.; Rodriguez, J.A.; Cooper, H.J. Modern trunnions are more flexible: A mechanical analysis of THA taper designs. *Clin. Orthop. Relat. Res.* **2014**, *472*, 3963–3970. [[CrossRef](#)] [[PubMed](#)]
33. Jacobs, J.J.; Gilbert, J.L.; Urban, R.M. Corrosion of metal orthopaedic implants. *J. Bone Jt. Surg. Am.* **1998**, *80*, 268–282. [[CrossRef](#)]

34. Osman, K.; Panagiotidou, A.P.; Khan, M.; Blunn, G.; Haddad, F.S. Corrosion at the head-neck interface of current designs of modular femoral components essential questions and answers relating to corrosion in modular head-neck junctions. *Bone Jt. J.* **2016**, *98*, 579–584. [[CrossRef](#)] [[PubMed](#)]
35. Cook, S.D.; Barrack, R.L.; Clemow, A.J.T. Corrosion and wear at the modular interface of uncemented femoral stems. *J. Bone Jt. Surg. Br.* **1994**, *76*, 68–72. [[CrossRef](#)]



© 2018 by the authors. Licensee MDPI, Basel, Switzerland. This article is an open access article distributed under the terms and conditions of the Creative Commons Attribution (CC BY) license (<http://creativecommons.org/licenses/by/4.0/>).